Development of a cryogenic system for the VIRUS array of 150 spectrographs for the Hobby-Eberly Telescope

Chonis, Taylor, Vattiat, Brian, Hill, Gary, Marshall, J., Cabral, Kris, et al.

Taylor S. Chonis, Brian L. Vattiat, Gary J. Hill, J. L. Marshall, Kris Cabral, D. L. DePoy, Michael P. Smith, John M. Good, John A. Booth, Marc D. Rafal, Richard D. Savage, "Development of a cryogenic system for the VIRUS array of 150 spectrographs for the Hobby-Eberly Telescope," Proc. SPIE 7735, Ground-based and Airborne Instrumentation for Astronomy III, 773576 (20 July 2010); doi: 10.1117/12.857362

SPIE.

Event: SPIE Astronomical Telescopes + Instrumentation, 2010, San Diego, California, United States

Development of a cryogenic system for the VIRUS array of 150 spectrographs for the Hobby-Eberly Telescope*

Taylor S. Chonis[a], Brian L. Vattiat[b], Gary J. Hill[b], J.L. Marshall[c], Kris Cabral[c], D.L. DePoy[c], Michael P. Smith[d], John M. Good[b], John A. Booth[b], Marc D. Rafal[b], Richard D. Savage[b]

[a]University of Texas at Austin, Department of Astronomy, 1 University Station, C1400, Austin, TX, USA 78712;
[b]McDonald Observatory, University of Texas at Austin, 1 University Station, C1402, Austin, TX, USA 78712;
[c]Texas A&M University, Department of Physics & Astronomy, 4242 TAMU, College Station, TX, USA 77843;
[d]University of Wisconsin, Department of Astronomy, 3321 Sterling Hall, 475 N. Charter Street, Madison, WI, USA 53706;

ABSTRACT

The upcoming Hobby-Eberly Telescope Dark Energy Experiment (HETDEX) has provided motivation for upgrading the Hobby-Eberly Telescope (HET) at the McDonald Observatory. This upgrade includes an increase in the field-of-view to accommodate the new and revolutionary Visible Integral-field Replicable Unit Spectrograph (VIRUS). VIRUS is the instrument designed to conduct the HETDEX survey and consists of 150 individual integral-field spectrographs fed by 33,600 total optical fibers covering the 22 arc-minute field-of-view of the upgraded HET. The spectrographs are mounted in four enclosures, each 6.0×3.0×1.4 meters in size. Each spectrograph contains a CCD detector that must be cryogenically cooled, presenting an interesting cryogenic and vacuum challenge within the distribution system. In this paper, we review the proposed vacuum jacketed, thermal siphon, liquid nitrogen distribution system used to cool the array of detectors and discuss recent developments. We focus on the design, prototyping, and testing of a novel "make-break" thermal connector, built from a modified cryogenic bayonet, that is used to quickly detach a single spectrograph pair from the system.

Keywords: Hobby-Eberly Telescope, VIRUS, Spectrograph, Liquid Nitrogen, Cryogenic, Vacuum

1. INTRODUCTION

The Visible Integral-field Replicable Unit Spectrograph (VIRUS[1–3]) is a novel new instrument consisting of at least 150 individual, simple integral field unit (IFU) spectrographs that will be used to carry out the Hobby-Eberly Telescope Dark Energy Experiment (HETDEX) using the Hobby-Eberly Telescope (HET) at the McDonald Observatory. HETDEX[4] will map ∼0.8 million Lyman-α Emitters from $1.9 < z < 3.5$ over a 420 degree^2 field (9 Gpc^3), using them as tracers for constraining dark energy and the expansion history of the universe. The ∼150 individual VIRUS spectrographs are built into 75 unit pairs. The ∼75 IFUs, each feeding a pair of spectrographs and containing 448 1.8 arcsec^2 fibers, are arrayed on the 22 arcmin diameter field of the HET after its wide-field upgrade (WFU[5,6]). The current status of the WFU is reviewed in Reference 7. VIRUS is a revolutionary instrument because its large scale multiplexing methodology is a possible solution to keeping ELT instrument costs under control.[1] Its simple design is extremely adaptable, and is used as the baseline design for the upgraded HET's new Low Resolution Spectrograph (LRS2[8]). Finally, it will be an extremely powerful HET facility instrument for additional science outside of HETDEX and provide a means of efficient spectroscopic follow-up for upcoming synoptic imaging surveys.[9]

*The Hobby-Eberly Telescope is operated by McDonald Observatory on behalf of the University of Texas at Austin, the Pennsylvania State University, Stanford University, Ludwig-Maximillians-Universität München, and Georg-August-Universität Goettingen

Further author information: (Send correspondence to T.S.C.)
T.S.C.: E-mail: tschonis@astro.as.utexas.edu, Telephone: 1-512-471-4475

Ground-based and Airborne Instrumentation for Astronomy III, edited by Ian S. McLean, Suzanne K. Ramsay, Hideki Takami, Proc. of SPIE Vol. 7735, 773576 · © 2010 SPIE · CCC code: 0277-786X/10/$18 · doi: 10.1117/12.857362

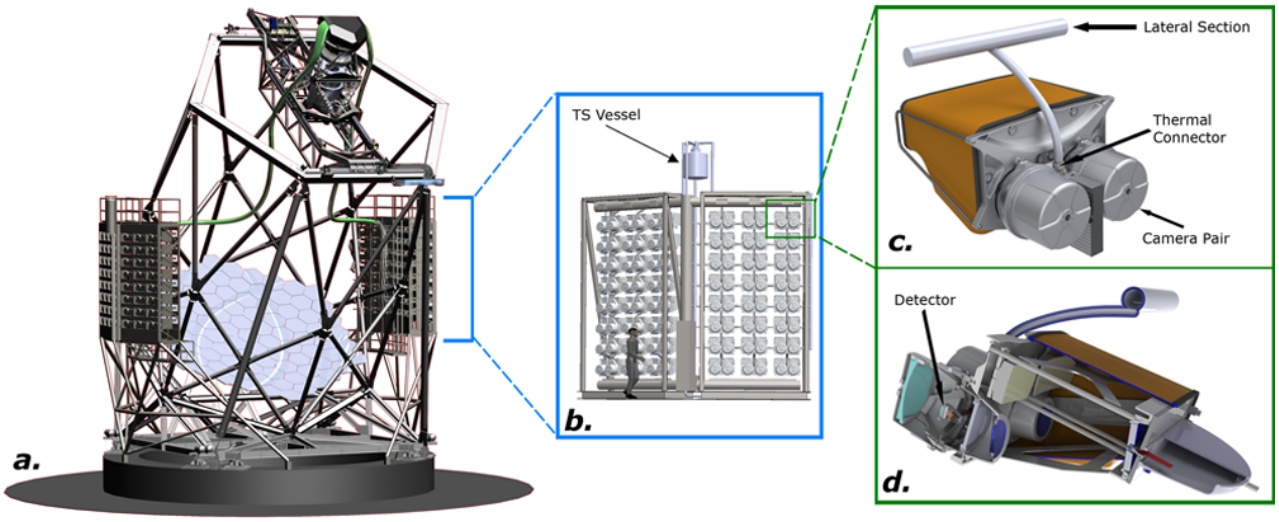

Figure 1. VIRUS mounted on the HET. *a*) A rendering of the HET after the WFU showing the four VIRUS enclosures mounted on the telescope structure. *b*) Close-up view of two out of four arrays of 8×3 VIRUS spectrographs, showing the LN_2 plumbing and TS Vessel described in Section 2. *c*) Detailed rendering of a single VIRUS pair. *d*) Section view of a single VIRUS pair.

In order to keep the fiber-optics feeding the spectrographs as short as possible (as needed to achieve the high UV throughput required for detecting Lyman-α Emitters in the redshift range required for HETDEX), the spectrographs will ride on the telescope structure in four separate environmentally controlled enclosures, each measuring 6.0×3.0×1.4 meters and placed ∼10 meters above the dome floor.[10] Figure 1 shows VIRUS mounted on the HET after the WFU. Light gathered by the HET primary mirror is directed into the prime-focus corrector optics and then into the IFU fiber-optics at f/3.65. The light then diverges out of the fibers into the spectrographs where it is collimated and dispersed into the camera by a VPH grating. The camera is of a Schmidt design and has its entire volume evacuated with the corrector plate acting as the cryostat window. By the Schmidt design, the detector is located at the prime-focus of the camera's mirror and is mounted in thermal isolation from the rest of the camera on a spider. The spectrograph and camera optics are described in detail in Reference 11. A series of copper cryogenic components provides the thermal link between the detector and the cold source. A prototype of a single VIRUS spectrograph (VIRUS-P[12]) has been constructed and in successful operation at the Harlan J. Smith 2.7 m telescope at McDonald observatory since 2006. The cold source for VIRUS-P is a simple liquid nitrogen (LN_2) filled dewar with a copper cold finger. While this simple approach is effective for a single spectrograph, it is unreasonable for the full VIRUS array of ∼75 unit pairs. In collaboration with Applied Cryogenics Technology, Inc. (ACT), McDonald Observatory developed a design study[13] to investigate the best way to cool the array of detectors. As outlined by Smith et al.,[14] the most effective cooling solution is a vacuum jacketed (VJ), thermal siphon (TS) LN_2 distribution system. This design is currently being developed in preparation for the completion of VIRUS.

We begin in Section 2 by concisely reviewing the LN_2 distribution system as outlined by Smith et al.[14] We then proceed in Section 3 to discuss the testing of a prototype "make-break" thermal connector that is integral to the design requirements of the system, followed by a discussion of the design and testing of a connector production model. We will then discuss the integration of this component into a VIRUS camera pair in Section 4, including a description of additional prototyped cryogenic components, the camera vacuum vessel, and a fully integrated test of the camera pair cryogenic system. Finally, we end in Section 5 with a description of further work in the near future that will be implemented to prove the remaining concepts of the LN_2 distribution system.

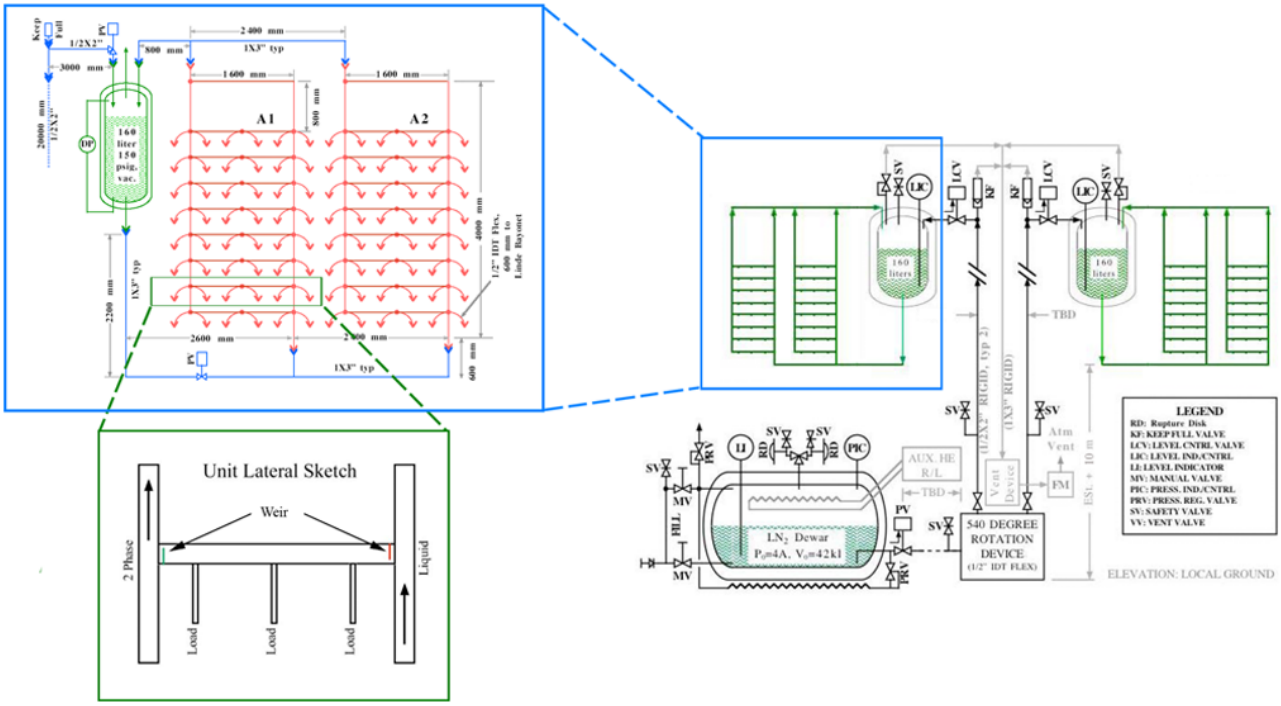

Figure 2. An overview schematic of the entire VIRUS cryogenic system. Detail is shown for the gravity fed thermal siphon system as well as for a single lateral in the manifold, showing the weir assembly. This figure is adapted from References 13 and 14.

2. OVERVIEW OF THE VIRUS CRYOGENIC SYSTEM

The baseline cryogenic system is described by Smith et al.[14] based on a collaborative design study with Mulholland.[13] The system will briefly be described here in order to put in context the details of prototyped components described in detail later in this work. Please refer to Figure 2, a schematic of the system, throughout the following description.

The VIRUS cryogenic system is a VJ, TS system which distributes LN_2 (T_{LN_2} = 75.3 K at McDonald Observatory's elevation; 77.4 K at 1 atm) to local thermal connectors at the spectrograph locations. The cold source for the system, which is common to all spectrographs, is an 11,000 gallon dewar located outside of the telescope dome where a truck-load of LN_2 is to be delivered roughly every other week. This source must deliver ~3600 W of cooling power after accounting for ~5 W per spectrograph, losses, and a 50% buffer. Through its own pressure created by nitrogen gas formation, liquid is forced from the storage dewar through a VJ transfer line which enters the telescope enclosure and connects to a flex line (via a cryogenic bayonet connection). The flex line serves the purpose of flexing with the telescope's azimuth rotation since the spectrographs are located on the telescope structure. At the end of the flex line, a connection is made to two VJ risers, which carry the coolant to the two 160 L TS vessels, one on each side of the telescope. The TS vessels, each given a continuous supply from the large storage dewar, supply the LN_2 to manifolds in a gravity feed where eight lateral lines of three thermal connections for spectrographs are located. There are a total of four manifolds, where each TS vessel feeds two. Nitrogen leaves the manifold in two phases, liquid and gas, after the heat loads on the thermal connectors in each lateral causes vaporization of some of the liquid. Each lateral utilizes weirs to prevent gas from entering the liquid risers and directing it through the two-phase return risers. The liquid and two-phase risers meet a horizontal return line back to the TS vessel, where the liquid is returned to the gravity feed and the vapor is separated out to a gas exit line. The fate of the ~80 K vapor is currently unknown: its cooling potential may be utilized in cooling detector electronics or the vapor may be heated and vented outside the dome.

The design of the system with four manifolds provides 96 thermal connections for spectrographs from the

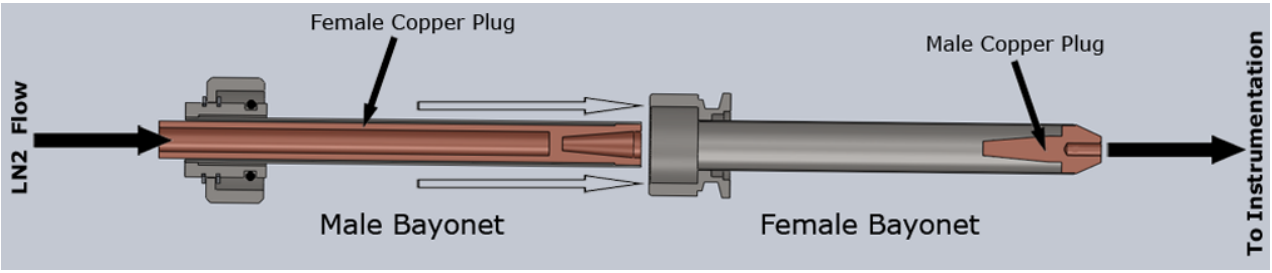

Figure 3. A schematic section view of the "make-break" thermal connector concept. A full description can be found in the text of Section 3.

laterals. This implies that the spectrographs are built in pairs, as previously mentioned, where each pair shares certain components (such as electronics, vacuum vessels, optics enclosures, and cryogenic components). Pairing spectrographs upholds the cost-efficient methodology with which VIRUS was designed as well as improving the use of the little available space on the telescope structure. Each of the thermal connections from the manifold lateral to the detector must provide efficient transfer of cooling power while providing a separation point so that an individual spectrograph pair can be removed from the system (e.g. for maintenance) without disrupting the cooling of the rest of the array. To achieve this, a closed connection (i.e. with no LN_2 flowing through) was devised by attaching a flexible, 0.5 inch ID VJ flex line from the lateral to a modified cryogenic bayonet in which custom copper thermal connectors are incorporated to provide the dry thermal connection. In the design study,[13] it was determined that this novel thermal connector was one of the highest-risk components in the system. As such, it has been prototyped and extensive testing has taken place. These tests and presentation of a production model are the subject of the next section.

3. THE THERMAL "MAKE-BREAK" CONNECTOR

The motivations for devising a "make-break", dry thermal connector for providing the thermal link between the coolant manifolds and the detector cold-fingers has been outlined in the previous section. In this section, we briefly describe the design of the connector, as first outlined by Smith et al.,[14] and then focus on its prototyping and testing.

The connector concept is based around a standard 3 inch (0.5 inch ID) Linde cryogenic bayonet, which is designed to connect two flex lines allowing direct flow of LN_2 between them. Since we do not desire direct flow through the connector, our modification is to add thermally conducting copper plugs to each side of the bayonet, which hinder the flow of LN_2 while transferring cooling power when in contact with each other. Figure 3 shows a schematic section cut of the connector. The female side of the standard bayonet is modified with a vacuum flange for attachment to the camera vacuum vessel. At the end of the female bayonet is where a male copper plug is brazed. The plug has an extrusion into the instrument where further cryogenic components, such as an activated charcoal getter and the detector cold finger, can be attached. Facing the opposite direction into the bayonet tube is a tapered extrusion where the thermal connection will be made. The male bayonet has a larger brazed female copper plug which contains two extruded cuts: one tapered for mating with the male copper plug and the other for providing ample surface area for contact with the LN_2. The inside of the VJ flex line from the manifolds carrying the LN_2 is brazed to the ID of the large extruded cut on the female copper plug allowing direct flow of LN_2 into it, thereby cooling the copper plug. The outside of the VJ flex line is welded to the OD of the male bayonet, sealing the VJ. When the two bayonet halves are brought together, the self-seating tapered extrusions make direct contact, thereby closing the thermal circuit and transferring the cooling power from the female copper plug to the male copper plug and then to the instrument. Using the VJ flex line allows flow of LN_2 into the connector, allowing the heat sink to be located right at the thermal connection and yielding the potential for the temperature gradient (ΔT) across the connector to be small. The connector concept depends on the LN_2 remaining in the nucleate boiling regime, where the liquid makes contact with the copper and boiling occurs in small, discrete bubbles from the surface. If the heat flux across the surface or ΔT is too large, the liquid moves to the sheet boiling regime where a layer of gas builds up between the liquid and the surface and no

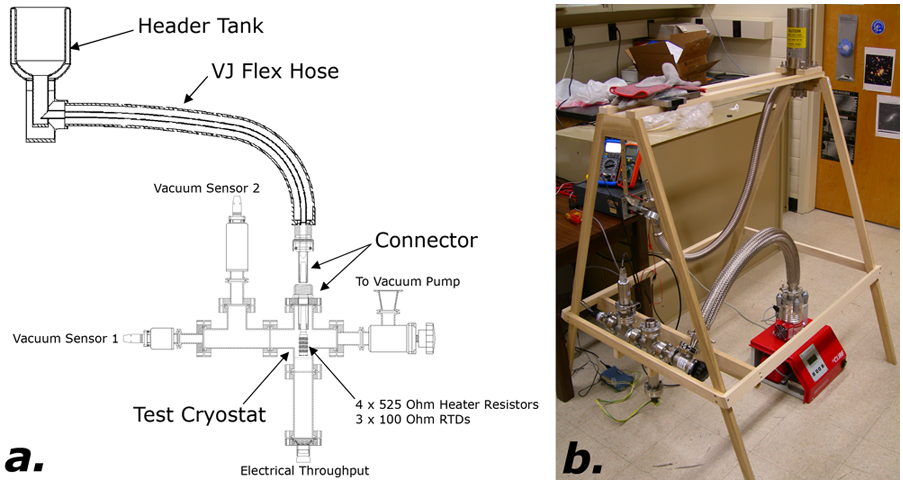

Figure 4. The apparatus for testing the prototype "make-break" connector. *a*) A schematic of the test apparatus and test cryostat. *b*) A photo of the apparatus assembled and mounted on its frame. Note that the female bayonet on the VJ flex line is positioned in the "gravity-switch" *off* position.

direct contact is made, reducing the cooling that can be achieved. For the 10 W cooling load of the camera pair, Smith et al.[14] report that at least 15 cm^2 of surface area for contact with LN_2 is needed to avoid sheet boiling. Note that for proper cooling operation, the bayonets must be oriented vertically with the LN_2 side (i.e. the male bayonet) on top so that gas escapes upward through the VJ line and into the manifold where it is then carried out and vented as described in Section 2. Turning the male bayonet upside-down results in a "gravity-switch" or "vapor-lock" as described and shown in Figure 8 of Smith et al.[14] This permits a thermal connector to be isolated from the rest of the cooling system when a spectrograph pair is detached for maintenance.

3.1 Proof of Concept: A First Prototype

The concept described above has been extensively tested to prove its functionality. In order to test the "make-break" connector, a test apparatus was constructed by Ability Engineering Technology, Inc. with a VJ gravity feed header tank and a 48 inch run of VJ 0.5 inch ID flex line. The flex line is attached to the first prototype male bayonet, containing the heat sink. A schematic of this basic gravity fed system can be seen in Figure 4*a*. The first prototype bayonet was constructed with a standard 3 inch Linde bayonet from Precision Cryogenics Systems, Inc. The female side, which is attached to a test cryostat constructed of standard 2.75 inch ConFlat vacuum components, has a long copper plug with a cylindrical extrusion containing four through-holes where four 525 Ω heater resistors are epoxied and tied together in parallel. At the end of the cylindrical extrusion is where three 100 Ω RTDs are located. Each of the RTDs is of a different brand and type following the IEC751 standard. Testing was performed on them to determine the best model for our purposes. We find that the most suitable sensor is a platinum thin-film 100 Ω RTD by Heraeus; all temperature values reported here are measured using this RTD model. The test cryostat also has locations for two vacuum sensors allowing testing of different sensor models to be carried out. These models will be discussed in Section 4.1. A schematic of the test cryostat can also be seen in Figure 4*a*. The entire apparatus is placed on a mounting frame which holds the location of the thermal connection a distance below the height of the header tank while maintaining that the connector remains in the proper vertical operational orientation. A photo of the mounted apparatus can be seen in Figure 4*b*. In this orientation, the header tank is filled with LN_2 from the top, which then flows into the VJ flex line. Once it reaches the female copper plug in the male bayonet, the LN_2 boils and the vapor returns through the flex line where it escapes into the air.

In these tests, we wish to learn the following: 1) if a single 0.5 inch ID flex line can simultaneously supply LN_2 to the heat sink and carry away the boil-off vapor; 2) at what power load does sheet boiling occur; and 3) general performance of the connector as a function of power. The following subsections describe the tests of the prototype.

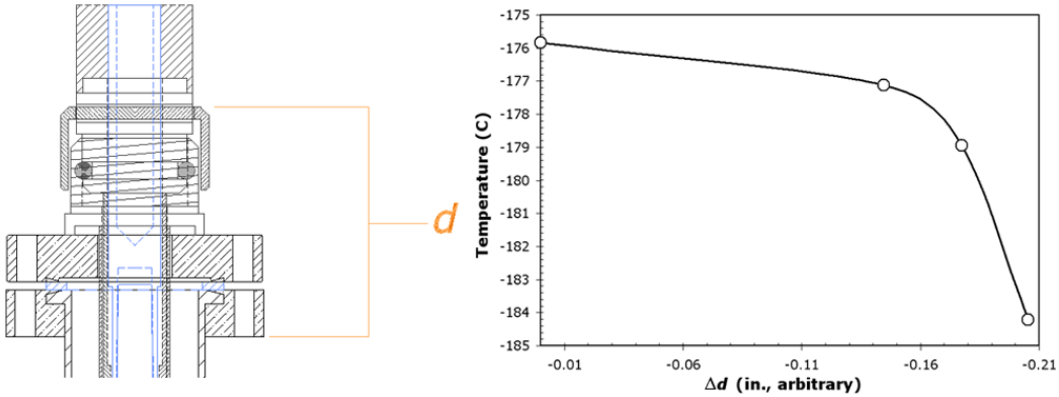

Figure 5. A plot of CET as a function of Δd. The force placed on the thermal connection is some function of Δd. Also shown is a schematic of the connector outside of the test cryostat showing how values of d are measured.

3.1.1 Reaching Temperature Equilibrium

Upon filling the header tank with LN_2, a large amount of boil off occurs and continues to do so until the heat sink is cooled down sufficiently to enter into nucleate boiling. We define the "cold equilibrium temperature" (CET) as the lowest constant temperature measured at the male copper plug in the female bayonet with no external load other than the bayonet itself. We consider a run of temperature as constant if $\Delta T/\Delta t < 0.04$ on average over a 5 minute period, where T is in units of degrees Celsius or Kelvin and t is in units of minutes. This is typically a good estimate of the true asymptotic temperature to within 1° Celsius. From room temperature, it takes ∼30 minutes for the system to reach CET. The average value of CET through all of our 3-inch prototype tests is 87.0±0.4 K, resulting in $\Delta T = 9.6 \pm 0.4$ K. With no external load other than the power losses in the bayonet itself, cooling to a sufficient level can be achieved with the prototype. The system quickly comes to equilibrium after a small change in load. After turning on the heaters (which adds additional load to the bayonet's intrinsic losses), the system reaches equilibrium at a higher temperature in ∼10 minutes on average.

We have also tested the "gravity-switching" process. After the apparatus was cooled to CET, the male bayonet was removed and hung upside-down, creating a "vapor-lock" (see Figure 4*b* in this work or Figure 8 of Smith et al.[14]). The vapor-lock was created and the male bayonet warmed back to ambient room temperature in ∼120 minutes. Subsequent cool down occurs on the timescale discussed in the above paragraph. A significant amount of frost will build up on the exposed bayonets while they are warming. See Section 3.1.2 for the effect of frost on the functionality of the connector when re-seating after a vapor-lock.

The mating copper plug extrusions are dimensioned so that they fully seat before the bayonet connection bottoms out, allowing a quantifiable amount of force to be placed on the thermal connection. More force can be placed on the thermal connection by tightening the bayonet. We expect the heat transfer to improve as more force is placed on the connection. For a simple test of this hypotheses, we assume that the force on the bayonet is some function of the distance from some arbitrary point on the test cryostat to the top of the knurled cap on the male bayonet that screws down onto the threaded portion of the female bayonet (see the schematic in Figure 5). We begin by seating the bayonet and lightly tightening the cap until a small amount of resistance is noticed. The quantity d in the schematic of Figure 5 is measured; we call the first reference measurement d_0. A corresponding temperature is also recorded. We then tighten the cap, which places more force on the thermal connection, and re-measure d. We calculate $\Delta d = d - d_0$ and record another temperature. In doing this multiple times, we are able to plot the run of temperature with Δd, which can be seen in Figure 5. Given that ∼8° Celsius of improvement in CET is observed in only ∼0.05 inch change in d shows that fully tightening the bayonet results in the best heat transfer and is necessary for proper operation.

3.1.2 Heater-Curve Tests

It is important to quantify both the power losses intrinsic to the bayonet as well as the change in temperature per input watt of power of the heaters. These values can be measured directly by plotting the temperature as

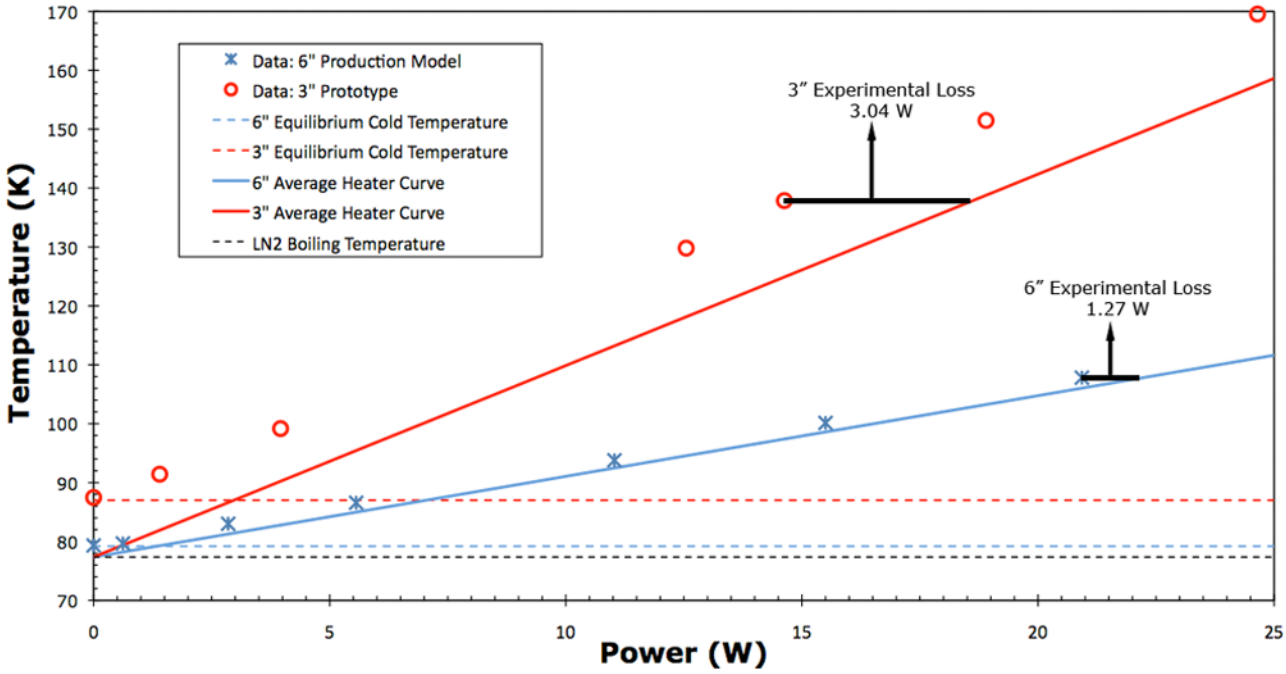

Figure 6. A temperature vs. power "heater-curve" plot. Red plots are for the 3-inch prototype bayonet described in Section 3.1. Blue plots are for the 6-inch production model described in Section 3.2. The data points are an example of a single heater-curve test and are uncorrected for bayonet losses. Horizontal dotted lines indicated specific temperatures of interest. The two solid lines are the calculated average heater-curves. The bayonet losses for each model are also indicated.

a function of power input into the system, referred to as a "heater-curve test". In normal nucleate boiling, we expect this relationship to be linear and for the linearity to break down (or at least for the slope to change) when entering the sheet boiling regime. The slope of the line gives the temperature change per input watt. The connector's losses can be derived by looking at the line's intercept. In an ideal system with no losses, the intercept of the heater-curve should pass through T_{LN_2}. That is, with no power losses, the male copper plug should ideally be at LN_2 boiling temperature. Since the connector is not ideal, it will not fulfill this requirement and its raw data will not have an intercept of 77.4 K. We then shift the raw data on the horizontal (Power) axis to force the intercept to be T_{LN_2}; the amount of shift is the total experimental power loss through the "make-break" connector in Watts.

The power input into the system P is calculated by measuring the current I through the resistors and the input voltage V and using the simple $P = VI$ relation. We avoid using the equivalent resistance of the resistors in the calculation as it is slightly temperature dependent. For each change in input power, a temperature measurement is made. Sample raw data for the 3-inch bayonet heater-curve test is shown in Figure 6 (red data points). The average CET indicated in Section 3.1.1 is also plotted as a red horizontal dotted line. We completed 14 such tests of the 3-inch prototype. The average heater-curve slope was 3.3±0.1 K/W while the experimentally determined loss in the connector is 3.04±0.08 W. The average heater curve is also plotted in Figure 6 as a solid red line and the loss determination is indicated.

Several modifications were added to the heater-curve test in an attempt to intentionally improve or degrade performance. The first was to perform a heater-curve test normally, then use the "gravity-switch" to turn the connector *off*. We then re-seat the connector, allow time to reach CET, and perform another heater-curve test to look for changes. No changes in performance after the gravity-switch were observed. We also perform this gravity-switch test and re-seat the bayonet while it is still cold. By blowing on the copper plugs, we introduce copious amounts of frost to each side. We then re-seat the bayonet and perform another heater curve test. It was hypothesized that the frost acts as an insulator, degrading the performance of the connector. This was falsified

as we observe identical behavior, even with frost present. In an attempt to improve the thermal conductivity of the connector, we added Apiezon N Cryogenic Vacuum Grease to each copper plug where the mate is located before performing a heater-curve test. The results with the conducting grease gave slightly improved results as compared to tests without grease. The improvements were slight however, indicating that the mate between the tapered copper components is solid. The grease did make it much more difficult to unseat the bayonet while still cold.

The fact that the connector cools down to give $\Delta T \sim 10$ K means that the LN_2 must be in a nucleate boiling state. In order to test where this breaks down and the heater-curve becomes either non-linear or discontinuous, we tested the connector to higher powers exceeding 25 W (i.e. >2 times the required power of a camera pair including bayonet losses). No breakdown in linearity or discontinuity is observed up to 25W as can be seen by the sample raw data in Figure 6. All of these results point toward a robust and successful prototype of the "make-break" connector concept. It can be seen that cooling of a VIRUS pair can be achieved with such a connector. Improvements on this design and subsequent testing will be discussed for a production model in the following section.

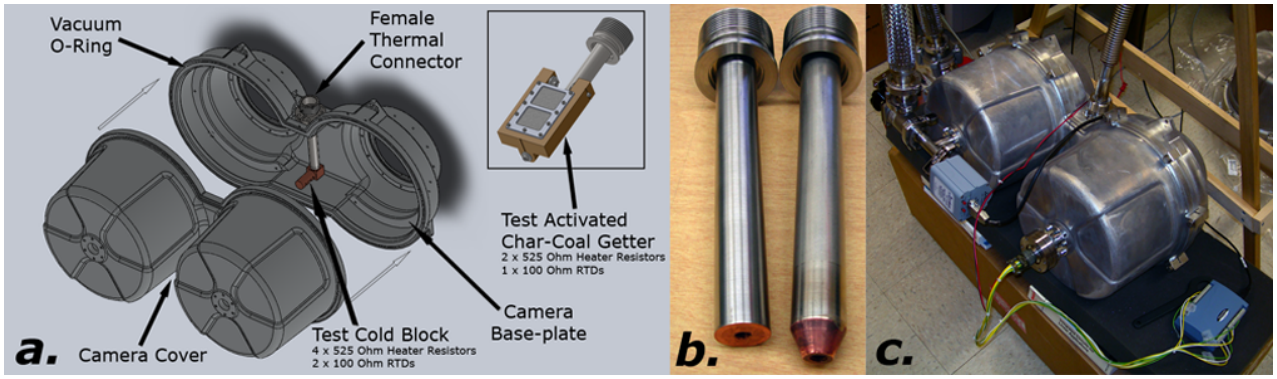

Figure 7. The test cryostat for testing the 6-inch production model connector. *a*) Exploded view of a prototype VIRUS camera vacuum vessel casting showing the 6-inch bayonet and test cold block where RTDs and heaters are mounted. Inset: the prototype activated charcoal getter, which takes the place of the test cold block in more recent tests, is shown attached to the female bayonet. *b*) Tapered and flat male copper plug ends. The flat end is used when mounting the prototype getter. *c*) A photo of the 6-inch test cryostat setup. Note the attached thermal connector.

3.2 6-Inch Production Model

While the 3-inch prototype was a success, the design can be improved upon. From a practical mechanical design standpoint, using a 6-inch bayonet makes logistical sense (see Vattiat et al[15] for a description of the evolution of the VIRUS mechanical design). Additionally, a longer bayonet allows the depth of the large extruded cut on the female copper plug into which LN_2 flows to be deeper, which increases the surface area onto which the LN_2 can make contact, reducing losses. We have also changed the design of the tapered extrusions to have a slightly steeper taper to facilitate self-seating. The 6-inch bayonet was also reverse engineered for our custom application and fabricated by our machine shops rather than modifying a standard bayonet.

To test the 6-inch bayonet, we have modified the test apparatus used for the testing the 3-inch prototype. The 3-inch male bayonet was removed from the VJ flex line and was replaced with the 6-inch male bayonet. Due to the larger size of the 6-inch bayonet, we have changed the test cryostat made from standard vacuum fittings. As will be discussed in Section 4.1, we have procured a set of prototyped, cast vacuum vessels for the camera pair. It was natural to utilize these prototypes to test the vacuum while also testing the 6-inch bayonet. We outfitted the end of the 6-inch bayonet with a test cold block. Like the 3-inch prototype, the test cold block has four bored holes for mounting heater resistors and an area where RTDs can be mounted. See Figure 7*a* for a model of the new test cryostat and 7*c* for a photo of the test cryostat with the connector assembled.

We find that the performance of the 6-inch model is greatly improved over the 3-inch prototype. The time to reach CET is shorter and measured to be 19 minutes. The average CET is 79.20±0.03 K, yielding ΔT = 1.80±0.03 K, implying that the power losses in the bayonet are quite small. We have conducted six heater-curve tests with this system. In these tests, we find a slope of 1.37±0.06 K/W and an experimental bayonet power loss of 1.27±0.07 W. In all respects, the 6-inch model is a vast improvement over the 3-inch prototype. The heater-curve tests are represented in Figure 6 in the same manner as for the 3-inch prototype. Given the larger surface area of the heat sink, reaching sheet boiling will be even more difficult with the 6-inch model, yielding consistent and reliable cooling.

We introduced similar modifications to the 6-inch tests as for the 3-inch prototype, including frost and gravity-switching. No change in performance was noticed with these modifications. As described by Vattiat et al.,[15] a necessary mechanical modification was made to the VIRUS enclosure design which tilted the spectrographs forward by 20°, meaning that the bayonet would no longer be perfectly vertical. We have tested the thermal connector in this configuration and found no change in performance since the slight angular tilt is not steep enough to affect the gravity feed. We theorize that the slight tilt may actually aid in allowing boiled-off vapor to escape, ensuring that the LN_2 reaches the heat sink unobstructed. For an additional modification, we have replaced the test cold block with a prototype of an activated charcoal getter which is used to maintain a good vacuum and was outfitted with RTDs and heaters (see the inset of Figure 7*a*; the affect of the getter on the vacuum is discussed in Section 4.1). We also modified the tip of the copper plug on a second female bayonet from tapered to flat, which makes machining the getter frame and copper plug simpler (see Figure 7*b*). Subsequent testing of the modified system gave a CET of 80.5 K, yielding ΔT = 3.1 K. The heater-curve slope is 1.45 K/W with a total loss of 2.11 W. While the performance of this modification is slightly degraded from the original 6-inch model, it is still more than adequate for our purposes and still an improvement over the 3-inch prototype. Given also that we used a different female bayonet with the same male bayonet, the fact that we observe acceptable test results shows that a given thermal connector port on the manifold is not unique to a specific spectrograph pair. We adopt the 6-inch version of the thermal "make-break" connector as the production model for VIRUS.

4. CRYOGENICS IN A CAMERA PAIR

As previously described, the spectrographs are to be constructed in pairs so that a given pair shares a single IFU, optics enclosure, and a common cryostat.[1] While this is largely driven by the handling of the fiber-optics, it is beneficial in terms of number and cost for the cryogenic system at the level of individual camera pairs while also improving the vacuum hold time due to the larger enclosed volume. Each camera in a pair shares a common vacuum vessel as well as a common thermal connection, which will yield cost savings for vacuum and cryogenic

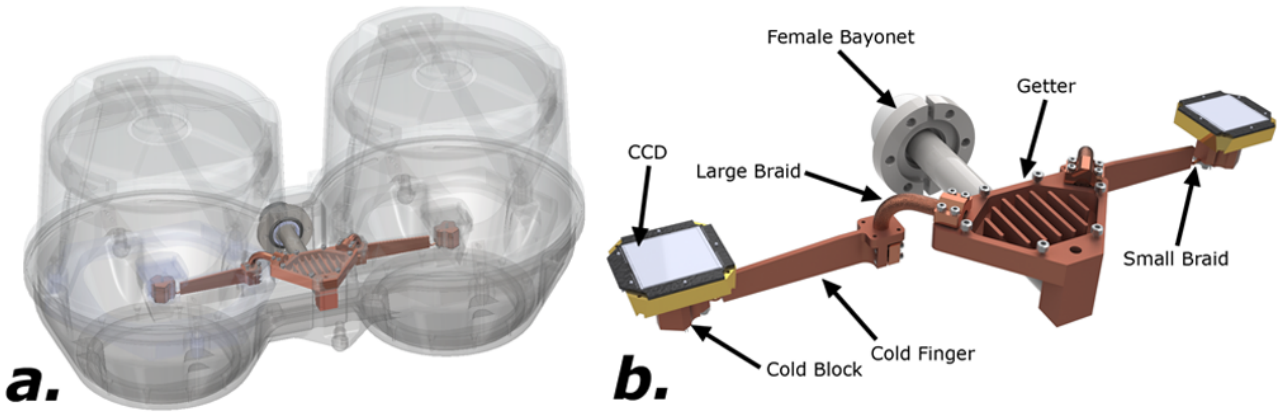

Figure 8. Cryogenic components inside of a VIRUS camera pair. *a*) Camera pair cryogenic components are shown highlighted as installed in a vacuum vessel. *b*) Camera pair cryogenic components shown in isolation with components labeled for reference in Section 4.

fixtures. Inside of a camera pair, the female side of the thermal connector described in Section 3 is attached to an activated charcoal getter, which is housed in a large copper fixture. The components for transferring cooling power to each detector are commonly attached to the getter fixture. For each detector arm, a large copper braid connects the getter fixture to a cold finger that runs through the arm of the spider which holds the detector at the prime focus of a spherical mirror inside the Schmidt camera. A smaller copper braid attaches the cold finger to a cold block establishing the thermal connection to the CCD detector. The camera's internal cryogenic components can be seen in Figure 8. In the following sections, we discuss the cryogenic system inside of a camera pair. We begin by discussing the vacuum vessels in which the components are housed and end with a discussion of a fully functional test assembly of the camera cryogenic system.

4.1 Vacuum Vessels

Since up to 96 spectrograph pairs are to be fabricated and constructed, it is necessary to work in a cost effective manner. As a result, we have explored and are utilizing castings for many mechanical components.[15] Of interest in this discussion is the cast vacuum vessels enclosing $\sim$37 L of volume in which the camera and cryogenic components will be housed. An exploded view of the cast aluminum vacuum housing and a photo of the casting in use for the 6-inch thermal connector tests can be seen in Figure 7*a* and 7*c*, respectively. Castings are typically not thought of as good vacuum chambers since their surfaces are somewhat porous as a result of the casting process.[15] MKS Instruments, Inc., to whom the prototype vacuum chamber castings were contracted, have used Loctite Resinol RTC (a liquid sealant designed for sealing porosity in castings) to impregnate the casting walls and seal any pores or other incursions. Each vacuum chamber consists of two large components: a camera base-plate and a camera cover. The fixtures which hold the camera optics are attached to the base-plate which then attaches to the spectrograph optics enclosure behind the diffraction grating. Light enters through a window which seals the vacuum on the base-plate and also serves as the Schmidt corrector plate. The base-plate also contains a large groove for an O-ring and a KF25 vacuum flange where the cryogenic bayonet is installed. The cover is a large hollow casting which mounts onto the base-plate and contains two KF25 vacuum flanges: one for a small vacuum pump-out valve and the other for the attachment of a pressure sensor.

We have tested the vacuum chambers to inspect the effectiveness of the Loctite Resinol RTC in a semi-high vacuum (e.g. $\sim 1\times10^{-6}$ Torr, which is the specified operating pressure in the VIRUS cameras) and tested the vacuum's sustainability in the presence of the prototyped getter. In the cost saving methodology of VIRUS, we have also explored methods of vacuum leak detection based on detecting conduction through a degrading vacuum. In the following tests, we have used the cast aluminum vacuum chambers described above in combination with an MKS Instruments, Inc. model 925 and 972 vacuum gauges (a model 999 gauge was also used on loan from MKS for some tests). We also utilize a small Pfeiffer Vacuum HiCube 80 Eco pumping station, which can achieve 67 L/s pumping speed for N_2. This pump is especially interesting because it is small and light (17 kg), allowing for easy transport inside the HET dome when maintaining VIRUS vacuum chambers that are located $\gtrsim$10 m above the dome floor. With this pump, we are easily able to pump out the $\sim$37 L volume of the camera vacuum vessels to a pressure of $\sim10^{-5}$ Torr in < 2 hours, depending on the conduction of the valve being used. With the vacuum vessels carefully cleaned and with various electrical and cryogenic components enclosed (which act as sources of out-gassing), the pressure in the chambers remains quite constant, rising $\lesssim$0.1 mTorr in over a week's time after pumping down to $\sim10^{-5}$ Torr. Additional He leak tests also show no obvious leaks and point towards a well maintained vacuum. With a prototyped activated charcoal getter installed and cooled, we are routinely able to achieve and maintain pressures between 10^{-6} and 10^{-7} Torr, which is adequate for the VIRUS vacuum specification.

While vacuum sensors are necessary for monitoring the vacuum in our test cryostats, we have explored whether there is a need for them on the VIRUS cameras. Since there are potentially up to 96 individual cryostats, eliminating the need for vacuum sensors would be a major cost-saver. We thus attempt to use the camera cryogenic system itself as a vacuum sensor which detects an increase in conduction as a result of an increasing density of gas molecules. In normal operation, the heaters regulate the temperature of the CCD detectors to -100° Celsius. If the camera pair's vacuum begins to degrade, thermal conductivity will increase, adding a heat load to the system and requiring less power for the heaters to hold the detectors at a constant temperature. This change in heater power ΔP could be detected and trigger a warning for a given camera pair to be serviced. In order to test this theory, we hold the power to the heaters constant while the pressure

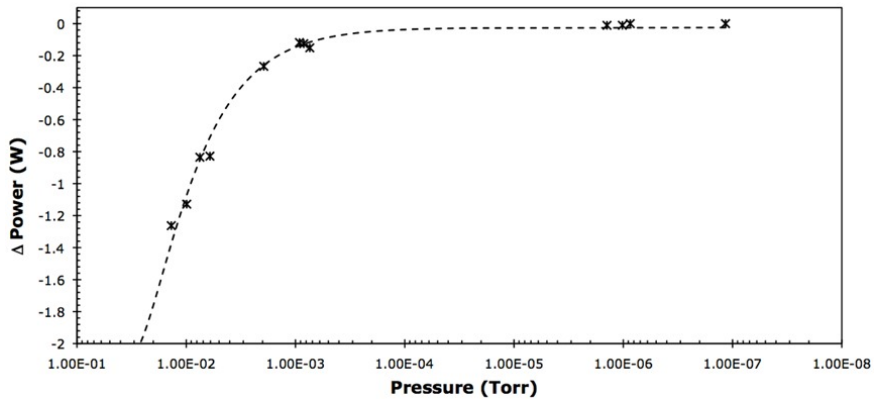

Figure 9. The change in power ΔP required to hold the temperature in a cryostat constant as a function of pressure.

in the cryostat is varied. With each change in pressure, a temperature reading is taken. This temperature is converted into a power using a heater-curve for which data was gathered directly before the vacuum was varied. The difference in power ΔP between the constant power given to the heaters and the power calculated for each temperature measurement is calculated and plotted against pressure. This plot can be seen in Figure 9; the data points shown were taken in three runs of the described test. The dearth of data points between 10^{-3} and $5{\times}10^{-5}$ Torr is a result of the vacuum "running-away" as the density of molecules becomes low enough to begin freezing-out onto the cryogenic surfaces in significant numbers, reducing the pressure too quickly for any data to be taken. As can be seen, $\Delta P \approx 0$ for all pressures $<10^{-3}$ Torr. No significant change in the required heater power is noticed until $\sim 5{\times}10^{-2}$ Torr, at which point the vacuum in the camera has already been significantly compromised. We therefore determine it necessary to equip the VIRUS camera cryostats with vacuum sensors so that leaks and other issues can be noticed and solved promptly. We have chosen the MKS 925 MicroPirani vacuum sensor as a suitable candidate for VIRUS thanks to its compact size, affordable price, and ability to measure pressures to 10^{-5} Torr.

4.2 Integrated Tests of the Camera Cryogenic System

We have constructed a test apparatus that will allow us to test the cryogenic system of an entire camera pair under realistic thermal loads. Astronomical Research Cameras, Inc. (ARC), to which the VIRUS detectors have been contracted, has provided us with a pair of mock CCD detectors which are mechanically identical to the actual detectors. The following describes the test apparatus built around these mock detectors which allow us to verify the thermal load of a camera pair and prove the functionality of internal cryogenic components.

4.2.1 Prototyped Components

The test apparatus for the integrated testing of camera pair cryogenic components can be seen in Figure 10. For this setup, we have prototyped the latest design for the activated charcoal getter, the cold finger, and the cold block onto which the mock CCD detector is mounted (see Figure 8*b* for the location of these components). These components have been connected via flexible copper braids which allow the relative mechanical isolation of the CCD detector from the rest of the cryogenic components. We have also used the base-plate half of the cast vacuum chamber as well as the 6-inch production thermal connector described in Section 3.2. The cold finger is mounted inside of a post-machined prototype invar spider, which is securely attached to the base-plate. For these tests, we have replaced the camera cover half of the cast vacuum chamber with a large plate containing windows over each CCD. In the future, these windows will allow for testing the amount of deflection of the spider arm though a cool-down/warm-up process utilizing lasers; this is beyond the scope of the present paper, however. Each cold block will be outfitted with a dedicated RTD and set of heater resistors; neither of these was installed at the time of this writing.

The following section will outline the results of our initial tests with this apparatus. Although the cryogenic component of the camera pair was complete at the time of this writing, the final setup with the CCD electrical

Figure 10. Assembly for integrated testing of camera pair cryogenics. *a*) Solid model of the integrated test assembly showing the large vacuum plate with windows installed cut away, revealing internal components. *b*) A photo of the integrated test assembly and vacuum plate. *c*) A photo of the spider with installed cryogenic components showing the location of the various RTDs (*blue arrows*) used for testing ΔT across component junctions.

flex-circuit, instrument RTDs, and heater resistors was not. Our simple initial tests utilize six RTDs strategically placed along the thermal circuit allowing us to measure values of ΔT across component junctions. We are especially interested in ΔT across the copper braids, in particular the small braid connecting the cold finger to the cold block (since this is the thermal bottle-neck in the system). We have determined the effective diameters d_{eff} of the copper braids if they were solid copper wire. For the large braid, d_{eff} = 4.7 mm; d_{eff} = 1.2 mm for the small braid. The location of the RTDs can be seen in Figure 10*c* and is as follows: at the getter before the large braid, on the cold finger after the large braid, at the opposite end of the cold finger before the small braid, on the cold block after the small braid, on the CCD, and on the spider. We require that the CCD temperature is -140° Celsius with no external load, allowing ample load to be placed on the system by the heater resistors to regulate the CCD's temperature. This diagnostic will show us to what degree this requirement can be met and where we can make improvements if it is not.

4.2.2 Test Results

As would be expected given the larger mechanical load on the thermal connection, the time required to reach CET (as defined in Section 3.1.1) has increased significantly as compared to our basic bayonet tests; this time also varies for individual components in the camera cryogenic system. The getter reaches CET = -184.6° Celsius in 118 minutes while the CCD reaches CET = -125.4° Celsius in 266 minutes. This CCD CET is not up to our requirement, and solutions to this issue will be discussed in the ensuing paragraphs.

We have cooled the system four times thus far, each time data logging the cool down at different locations in the cryostat. The resulting average temperatures T as a function of time Δt can be seen in Figure 11. In all tests, the temperatures for the getter and cold finger were consistent. The CET of the cold finger after the large braid is -173.0° Celsius, resulting in ΔT = 11.6° Celsius across the large braid. ΔT across the length of the cold finger is 2.4° Celsius, indicating minimal radiation coupling between it and the spider. This is confirmed by the warm average temperature of the spider (-4.6° Celsius). The average value of ΔT for the CCD and cold block junction is 3.3° Celsius. All of these ΔT values are quite acceptable. As expected from its small cross-section, the small braid is the thermal bottle-neck in the system. Our initial tests had poor contact between the cold finger, cold block, and small braid. This can be seen by the curve in Figure 11 labeled as "CCD - d_{eff} (1)". Upon re-seating the braid by folding the ends before clamping (thereby increasing the amount of pressure the clamps can put on the braid and reducing contact resistance), we were able to increase the performance by ∼10° Celsius to the CET value quoted in the previous paragraph, resulting in a still large value for ΔT (45.7° Celsius). This curve is labeled in Figure 11 as "CCD - d_{eff} (2)". In order to reduce this value of ΔT, we aim to increase d_{eff} for the small braid. Since the cold finger would not accept a braid with $2d_{eff}$, we opted to use a solid piece of copper wire. AWG12 solid copper wire has a suitable diameter for fitting the cold finger in place of the braid while having a diameter that is $1.7d_{eff}$. This resulted in a much higher conductivity and a new CET of -151.1° Celsius was reached in 179 minutes (the new ΔT across the junction from the cold finger to the cold block is 15.4° Celsius). This performance is highly desirable, but with a flexible braid instead of a rigid wire, allowing

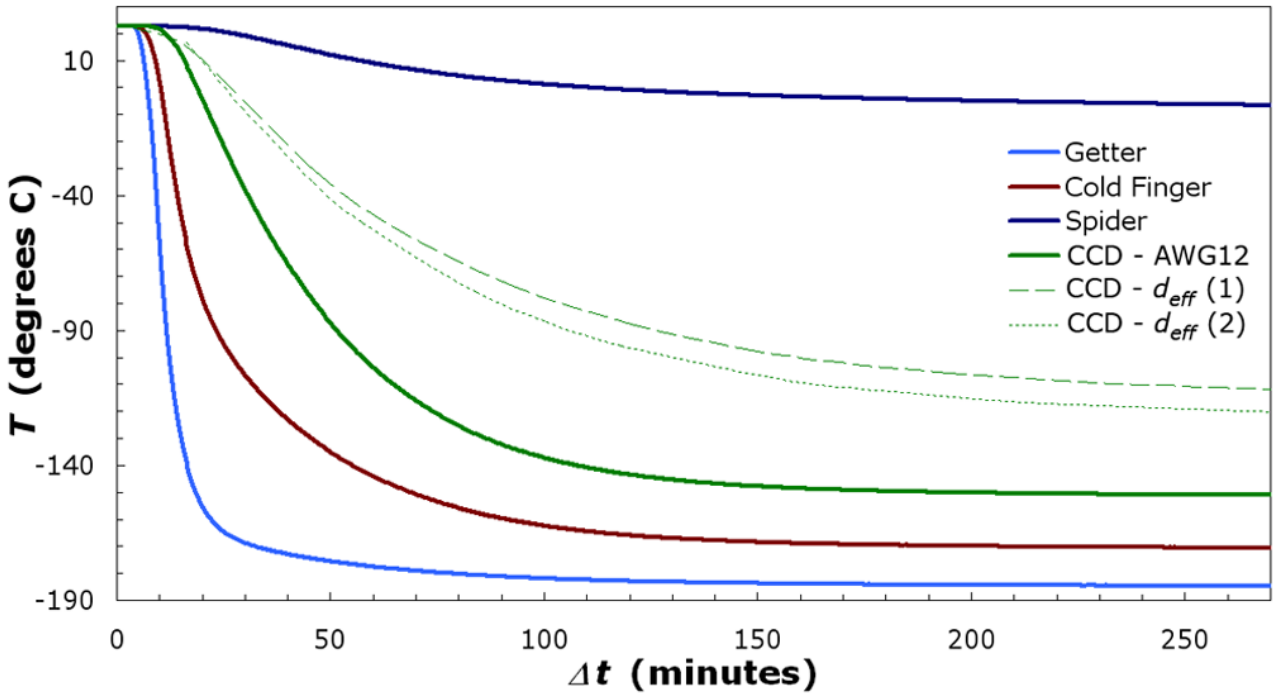

Figure 11. Temperature T as a function of time Δt during the cool-down process of the test camera pair cryogenics. Each curve represents T as recorded by an RTD at the indicated location. Three plots of temperature for the CCD are shown, each taken during a different test. The AWG12 designation indicates data for the test with the small braid replaced by solid AWG12 copper wire. d_{eff} (1) and (2) are data taken with the original small braid in place and are described in the text of Section 4.2.2.

a relative mechanical decoupling of the detector from the rest of the cryogenic system. Modifications must be made to the design of the cold finger before a larger braid with similar d_{eff} as AWG12 wire can be tested.

Using the heater-curve results for the 6-inch production thermal connector (see Section 3.2 or Figure 6), we can estimate the amount of heat load on the thermal connection as a result of cooling two full detectors (albeit without the external load of the regulating heater resistors). Including the inherent losses in the bayonet, we estimate a 9.2 W load on the thermal connection. The flex-circuit will add a few tenths of a watt to this total, along with the additional power required to regulate the CCD temperature. These first tests of an integrated cryogenic camera pair are quite encouraging. Given a larger braid for connecting the cold block and the cold finger and the modifications to accommodate such a braid, the CCD temperature with no external load will exceed our requirement. This apparatus will serve as a future test bed for mechanical testing at cryogenic temperatures as well as detector testing when actual CCDs arrive.

5. CONCLUSIONS & FUTURE WORK

In conclusion, we have presented an overview of the VIRUS cryogenic system as well as recent developments and prototyped components. The main development is the design, proof of concept, and testing of a thermal "make-break" connector, which was considered one of the highest-risk components of the cryogenic system. We have also procured and tested an entire assembly of the internal cryogenics for a camera pair.

Since the design concept has proven successful on the scale of an individual VIRUS unit, the natural next step in the development process of the cryogenic system is to begin multiplexing the tests described in this work. A design has been completed and fabrication of a 6 connector manifold (containing two laterals of three connectors each) fed by a header tank under TS is underway. We also aim to extend our cold tests of vacuum stability to longer time scales (on the order of months) in order to prove the endurance of the activated charcoal getter and

test the longer term stability of the cast aluminum vacuum chambers. With a fully integrated cryogenic test apparatus for a camera pair, we plan to test CCD temperature regulation as well as the mechanical effects of a cool-down on the camera (e.g. detector head deflection as a function of temperature). We also expect the first actual VIRUS detectors to arrive from ARC in the coming months. The CCDs must be cooled and regulated at operational temperatures in order to carry out detector tests, which will also allow further testing of the camera cryogenic test assembly in a much more realistic situation.

ACKNOWLEDGMENTS

HETDEX is led by the University of Texas at Austin McDonald Observatory and Department of Astronomy with participation from the Universitäts-Sternwarte of the Ludwig-Maximilians-Universität München, the Max-Planck-Institut für Extraterrestriche-Physik (MPE), Astrophysikalisches Insitut Potsdam (AIP), Texas A&M University, Pennsylvania State University, and the HET consortium. HETDEX is funded in part by gifts from Harold C. Simmons, Robert and Annie Graham, The Cynthia and George Mitchell Foundation, Louis and Julia Beecherl, Jim and Charlotte Finley, Bill and Bettye Nowlin, Robert and Fallon Vaughn, Eric Stumberg, and many others, by AFRL under agreement number FA9451-04-2-0355, and by the Texas Norman Hackerman Advanced Research Program under grants 003658-0005-2006 and 003658-0295-2007.

We thank the late George T. Mulholland of ACT for developing the conceptual design of the VIRUS cryogenic system, including the concept for the bayonet-based thermal connector. We also thank Richard Allen and Jimmy Welborn for help with the construction of some of the prototyped cryogenic components described and tested in this work.

REFERENCES

[1] Hill, G. J., Adams, J. J., Blanc, G., Booth, J. A., Chonis, T. S., Cornell, M. E., DePoy, D. L., Drory, N., Gebhardt, K., Good, J., Grupp, F., Kelz, A., Lee, H., MacQueen, P. J., Marshall, J. L., Mollison, N., Murphy, J. D., Rafal, M. D., Roth, M. M., Savage, R., Smith, M. P., and Vattiat, B. L., "VIRUS: a massively replicated 33k fiber integral field spectrograph for the upgraded Hobby-Eberly telescope," in [*Astronomical Telescopes and Instrumentation*], *Proc. SPIE* **7735-21** (2010).

[2] Hill, G. J., MacQueen, P. J., Tufts, J. R., Kelz, A., Roth, M. M., Altmann, W., Segura, P., Gebhardt, K., and Palunas, P., "VIRUS: a massively replicated integral-field spectrograph for HET," in [*Ground-based and Airborne Instrumentation for Astronomy*], *Proc. SPIE* **6269-79** (2006).

[3] Hill, G. J., MacQueen, P. J., Tejada, C., Cobos, F. J., Palunas, P., Gebhardt, K., and Drory, N., "VIRUS: a massively replicated IFU spectrograph for HET," in [*Ground-based Instrumentation for Astronomy*], *Proc. SPIE* **5492-251** (2004).

[4] Hill, G. J., Gebhardt, K., Komatsu, E., and MacQueen, P. J., "The Hobby-Eberly Telescope Dark Energy Experiment," in [*The New Cosmology: Conference on Strings and Cosmology; The Mitchell Symposium on Observational Cosmology*], *AIP Conference Proc.* **743-224** (2004).

[5] Booth, J. A., MacQueen, P. J., Good, J. M., Wesley, G. L., Hill, G. J., Palunas, P., Segura, P. R., and Calder, R. E., "The wide field upgrade for the Hobby-Eberly Telescope," in [*Ground-based and Airborne Telescopes*], *Proc. SPIE* **6267-128** (2006).

[6] Savage, R. D., Booth, J. A., Gebhardt, K., Good, J. M., Hill, G. J., MacQueen, P. J., Rafal, M. D., Smith, M. P., and Vattiat, B. L., "Current status of the Hobby-Eberly Telescope wide field upgrade and VIRUS," in [*Ground-based and Airborne Telescopes II*], *Proc. SPIE* **7012-9** (2008).

[7] Savage, R. D., Booth, J., Cornell, M., Gebhardt, K., Good, J., Hill, G. J., Lee, H., MacQueen, P. J., Perry, D., Rafal, M., Rafferty, T., Ramiller, C., C. Taylor, I., Vattiat, B. L., Beno, J., Beets, T., Hayes, R., Heisler, J., Hinze, S., Soukup, I., Jackson, J., Mock, J., Zeirer, J., Worthington, M., Mollison, N., Molina, O., South, B., Wardell, D., and Wedeking, G., "Current status of the Hobby-Eberly Telescope wide field upgrade," in [*Astronomical Telescopes and Instrumentation*], *Proc. SPIE* **7733-149** (2010).

[8] Lee, H., Chonis, T. S., Hill, G. J., DePoy, D. L., Marshall, J. L., and Vattiat, B. L., "LRS2: a new low-resolution spectrograph for the Hobby-Eberly Telescope and its application to scalable spectrographs for the future extremely large telescopes," in [*Ground-based and Airborne Instrumentation for Astronomy III*], *Proc. SPIE* **7735-276** (2010).

[9] Hill, G. J., MacQueen, P. J., Palunas, P., Barnes, S. I., and Shetrone, M. D., "Present and future instrumentation for the Hobby-Eberly Telescope," in [*Ground-based and Airborne Instrumentation for Astronomy II*], *Proc. SPIE* **7014-5** (2008).

[10] Heisler, J. T., Good, J. M., Savage, R. D., Vattiat, B. L., Hayes, R. J., Mollison, N. T., and Soukup, I. M., "Integration of VIRUS spectrographs for the HET dark energy experiment," in [*Ground-based and Airborne Telescopes III*], *Proc. SPIE* **7733-153** (2010).

[11] Lee, H., Hill, G. J., Marshall, J. L., DePoy, D. L., and Vattiat, B. L., "VIRUS optical tolerance and production," in [*Ground-based and Airborne Instrumentation for Astronomy III*], *Proc. SPIE* **7735-140** (2010).

[12] Hill, G. J., MacQueen, P. J., Smith, M. P., Tufts, J. R., Roth, M. M., Kelz, A., Adams, J. J., Drory, N., Grupp, F., Barnes, S. I., Blanc, G. A., Murphy, J. D., Altmann, W., Wesley, G. L., Segura, P. R., Good, J. M., Booth, J. A., Bauer, S.-M., Popow, E., Goertz, J. A., Edmonstron, R. D., and Wilkinson, C. P., "Design, construction, and performance of VIRUS-P: the prototype of a highly replicated integral field spectrograph for the HET," in [*Ground-based and Airborne Instrumentation for Astronomy II*], *Proc. SPIE* **7014-257** (2008).

[13] Mulholland, G. T., [*VIRUS Cryogenic System Design Study Task 1B Final Report*], Applied Cryogenics Technology, Ovilla, TX (2008).

[14] Smith, M. P., Mulholland, G. T., Booth, J. A., Good, J. M., Hill, G. J., MacQueen, P. J., Rafal, M. D., Savage, R. D., and Vattiat, B. L., "The cryogenic system for the VIRUS array of spectrographs on the Hobby-Eberly Telescope," in [*Advanced Optical and Mechanical Technologies in Telescopes and Instrumentation*], *Proc. SPIE* **7018-117** (2008).

[15] Vattiat, B. L., Bauer, S., Booth, J. A., DePoy, D. L., Good, J., Hill, G. J., Kelz, A., Marshall, J. L., Rafal, M., Savage, R., and Smith, M. P., "Mechanical design evolution of the VIRUS instrument for volume production and deployment," in [*Astronomical Telescopes and Instrumentation*], *Proc. SPIE* **7735-264** (2010).